Design rules for oxoporphyrinogen ('OxP') as a versatile chromophore for efficient singlet oxygen generation

Jan Hynek[a†], Mandeep K. Chahal[a†], Daniel T. Payne*[a,b†], Anuradha Liyanage[c], Francis D'Souza[c] and Jonathan P. Hill*[a]

[a]*International Center for Materials Nanoarchitectonics, National Institute for Materials Science, Namiki 1-1, Tsukuba., Ibaraki 305-0044, Japan*

[b]*International Center for Young Scientists, National Institute for Materials Science, Sengen 1-2-1, Tsukuba., Ibaraki 305-0047, Japan*

[c]*Department of Chemistry, University of North Texas, 1155 Union Circle, 305070 Denton, Texas 76203, USA.*

Received date (to be automatically inserted after your manuscript is submitted)
Accepted date (to be automatically inserted after your manuscript is accepted)

ABSTRACT: Meso-5,10,15,20-tetrakis-3,5-di-*tert*-butyl-4-oxocyclohexadienylideneporphyrinogen, **OxP**, is a versatile, highly colored chromophore with strong broad absorption in the visible range. It is derived from meso-5,10,15,20-tetrakis(3,5-di-*tert*-butyl-4-hydroxyphenyl)porphyrin by two-electron oxidation, and the **OxP** tetrapyrrole moiety exists in a saddle conformation. N-Alkylation of the **OxP** core nitrogen atoms can be used to functionalize the chromophore leading to a class of stable molecules with highly substituted peripheries. Substituted **OxP**s can act as singlet oxygen generators under light irradiation and the efficacy of this process is influenced by the multiplicity of N-substitution, and by the chemical identity of those substituents. Bromination of the macrocyclic β-positions can also be used to control singlet oxygen generation by the relevant derivatives. We report the quantum yields of singlet oxygen generation for a series of differently substituted **OxP** derivatives whose metrics indicate that these compounds possess significant potential in the corresponding applications including photodynamic therapy, bacterial inactivation therapy, and organic transformations.

KEYWORDS: Oxoporphyrinogen, porphyrinoid, singlet oxygen generator.

*Correspondence to: Daniel T. Payne, e–mail: Daniel.Payne@open.ac.uk; Jonathan P. Hill, e–mail: Jonathan.Hill@nims.go.jp, tel.: +81–29–860–4399.

†Current address: (J. H.): Institute of Inorganic Chemistry, Czech Academy of Sciences, 250 68 Husinec-Řež, Czech Republic; (M. K. C.): Department of Chemistry, University of Southampton, University Road, Southampton, SO17 1BJ, United Kingdom; (D. T. P.) School of Life, Health and Chemical Science, Open University, Walton Hall, Milton Keynes, MK7 6AA, United Kingdom

INTRODUCTION

Oxoporphyrinogen, **OxP**, is a highly colored tetrapyrrole chromophore obtained by the aerial oxidation of the porphyrin (**TDtBHPP**)[1] under acidic[2] or, more usually, basic conditions.[3] Redox transformations involving **OxP**/**TDtBHPP** have been studied revealing potential catalytic properties.[4,5] **OxP** and its N-alkylated derivatives exhibit broad electronic absorption across most of the visible range, undergo reversible redox processes,[6,7] and have a saddle-shaped macrocycle (similar but not identical to calix[4]pyrrole[8]), which facilitates electronic conjugation between its different component groups. The **OxP** chromophore is synthetically flexible with augmentation possible by simple N-alkylation,[6,7] variation of meso-substituents,[9,10,] and substitution at macrocyclic β-positions.[11,12] Available derivatives of **OxP** include multichromophore systems,[13,14] metal-organic frameworks,[15] simple N-substituted compounds,[6,7,16,] and the corrole analogue, **OxC**.[17] These compounds have variously been exploited for sensing applications,[18,19] as photosynthetic model systems,[20] and for self-assembly.[21]

Chromophores, such as **OxP,** with electronic structures that enable triplet excited states can interact with triplet state ambient dioxygen generating singlet oxygen ($^1O_2$).[22,23] Although as a reactive oxygen species (ROS), $^1O_2$ is often seen as a hazard, recently it has garnered increasing attention due to several possible applications such as in organic oxidative transformations,[24] amelioration of pollutants[25] (especially for water purification[26]) and most importantly in photodynamic therapy (PDT)[27] including bacterial inactivation[28] or cancer treatment.[29] PDT applications are based on the essential restricted oxidative properties of $^1O_2$ due to high reactivity (especially towards organic materials) and its moderate lifetime, so that selective tumor targeting becomes possible. Useful chromophore classes such as the phthalocyanines[30,31] have properties appropriate for the relevant applications with novel $^1O_2$-generating molecules now being discovered.[32] Activation by two-photon absorption is also available for *meso*-tetraphenylporphyrin[33] and its derivatives.[34] New materials are screened and can be assessed for their usefulness by direct comparison with an appropriate reference compound.[35] Many of the applications involving $^1O_2$-generating molecules including PDT are required to operate in aqueous media so water-soluble reference materials must be used. Despite this, the estimation of $^1O_2$ quantum yields (Φ_Δ) in other largely organic media might also be used to assess the usefulness of novel chromophores such as the relatively hydrophobic **OxP** derivatives. Several classes of compounds can be used as $^1O_2$-generators including C_{60} buckminsterfullerenes,[36] Rose Bengal analogues,[37] phenalenone[38] and tris(2,2′-bipyridine)ruthenium(II) salts ($Ru(Bipy)_3Cl_2$.[39] Here we report $^1O_2$-generation by a series of substituted OxP molecules where we have attempted to identify the key structural features required for the effective operation of the chromophore either as a $^1O_2$ generator in its own right, or for use as a reference material to be used in the assessment of other active materials. For the latter, OxP materials might be useful since they possess an intense absorbance in the visible region where many other relevant dyes absorb. In general, we found that per-N-substituted **OxP** derivatives are the optimum structural type for efficient $^1O_2$ generation while a variation of the N-substituents can also be used to optimize their activity.

MATERIALS AND METHODS

General. Reagents and dehydrated solvents (in septum-sealed bottles) used for syntheses and spectroscopic measurements were obtained from Tokyo Kasei Chemical Co., Wako Chemical Co. or Aldrich Chemical Co. and were used without further purification. Optical absorption spectra were measured using JASCO V-570 UV/Vis/NIR spectrophotometer. FTIR spectra were obtained from solid samples using a Thermo-Nicolet 760X FTIR spectrophotometer. ^{1}H NMR and proton decoupled ^{13}C NMR spectra were recorded on a JEOL JNM-ECS400 NMR spectrometer respectively at 400 MHz, and 101 MHz. For ^{1}H NMR, tetramethylsilane (δ = 0 ppm) was used as a reference while for ^{13}C NMR spectra the residual solvent peak was used as a reference. Data were processed on Delta version 5.0.5.1 and Always JNM-AL version 6.2. ^{1}H NMR chemical shifts (δ) are reported in ppm relative to TMS for $CDCl_3$ (δ 0.00) or the residual solvent peak for other solvents. ^{13}C NMR chemical shifts (δ) are reported in ppm relative to the solvent reported. Coupling constants (*J*) are expressed in Hertz (Hz), shift multiplicities are reported as singlet (s), doublet (d), triplet (t), quartet (q), double doublet (dd), multiplet (m) and broad singlet (bs). $^{1}O_2$ photoluminescence spectra were measured using an InGaAs NIR photodetector (R5509-73, Hamamatsu Photonics, Japan) on a NanoLog Horiba Jovin Yvon spectrofluorometer with a 450-W xenon lamp as an excitation source at room temperature. A right-angle detection method and quartz cuvettes with four optical faces and usable in the UV field were used for emission measurements. Compounds **OxP**,[1] **OxP(4BrBn)$_2$**,[40] **OxP(4BrBn)$_4$**,[40] **OxP(Bn)$_4$**,[6] **β-Br$_8$OxP,**[41] **β-Br$_8$OxP(4BrBn)$_2$**,[41] **β-Br$_8$OxP(4BrBn)$_4$**,[42] **OxP(4CO$_2$MeBn)$_4$**[15] were prepared and purified according to literature methods.

$^{1}O_2$ quantum yield measurements. Emission spectra and $^{1}O_2$ photoluminescence spectra were measured using an NIR photodetector (Hamamatsu Photonics, Japan) on a NanoLog Horiba Jovin Yvon spectrofluorometer with a 450 W xenon lamp as an excitation source at room temperature under ambient conditions (unless otherwise stated). To estimate singlet oxygen quantum yields, the solutions of compounds were absorbance normalized (*ca.* 0.17–0.19 a.u.) with the reference compound (C_{60} Buckminsterfullerene[43,44], $\Phi_{\Delta=1}$) at the relevant excitation wavelength (500 or 510 nm) in toluene. Quantum yields (Φ_Δ) were determined by comparison of the average $^{1}O_2$ photoluminescence maxima values of the reference (I_{ref}) and compound being studied (I_{sample}) between 1270-1275 nm after background subtraction using the formula:

$$\Phi_\Delta = \frac{I_{sample}}{I_{ref}} \times \Phi_\Delta^{ref} \quad (1)$$

Synthesis.

OxP(4NO$_2$Bn)$_4$

A round-bottom flask was charged with 2.00 g (1.77 mmol) of 5,10,15,20-tetrakis(3,5-di-tert-butyl-4-hydroxyphenyl)porphyrin and 710 mg (17.7 mmol) of sodium hydride. The solid reagents were dissolved in 500 mL of acetone and stirred for 15 min. After that, 9.2 g (42.6 mmol) of 4-nitrobenzyl bromide dissolved in 50 mL acetone was added. The mixture was heated under reflux. After 4 h, 9.2 g (86.8 mmol) of Na_2CO_3 was added and the reaction was heated for an additional 20 h. After cooling down the resulting suspension was filtered through a Büchner funnel and the solid residue was washed with CH_2Cl_2. The filtrate was collected and rotary evaporated. The solid residue was dissolved in a minimal amount of CH_2Cl_2 and precipitated with MeOH. The green solid was collected by filtration, washed with MeOH,

and vacuum dried. Yield: 2.46 g (83 %). UV/Vis (CH_2Cl_2): λ_{max} (ε, M^{-1} cm^{-1}) = 272 (73400), 492 (186000) nm. ^{1}H NMR (400 MHz, $CDCl_3$): δ 8.07 (d, J = 8.8 Hz, 8H), 7.20 (s, 8H), 6.80 (d, J = 8.4 Hz, 8H), 6.72 (s, 8H), 4.60 (s, 8H), 1.23 (s, 72H) ppm. ^{13}C NMR (100.5 MHz, CDCl3): δ 185.7, 149.4, 147.8, 144.1, 137.9, 134.9, 130.0, 127.9, 126.8, 124.3, 120.6, 47.9, 35.7, 29.4 ppm. FTIR (ATR): ν = 3111 (w), 3078 (w), 2997 (w), 2954 (s), 2910 (m), 2866 (m), 1711 (w), 1641 (w), 1591 (s, carbonyl C=O stretching), 1522 (s), 1489 (m), 1454 (m), 1402 (w), 1389 (w), 1360 (m), 1344 (s), 1325 (m) 1309 (s), 1257 (m), 1221 (w), 1200 (w), 1176 (w), 1111 (w), 1088 (m), 1043 (m), 1016 (m), 960 (w), 953 (m), 930 (m), 920 (w), 906 (w), 887 (w), 856 (m), 839 (m), 820 (m), 800 (s), 756 (w), 744 (w), 729 (s), 704 (w), 683 (w), 661 (w), 640 (w), 623 (m) cm^{-1}. HRMS: found: 1666.8492, calcd.: 1666.8551.

OxP(4NH$_2$Bn)$_4$

A round-bottom flask was charged with 1.00 g (0.60 mmol) of **OxP(4NO$_2$Bn)$_4$**, 3.00 g (12.5 mmol) of $Na_2S{\cdot}9H_2O$ and 300 mg (5.60 mmol) of NH_4Cl. The flask was three times evacuated and purged with N_2. The reagents were dissolved in 120 mL of N_2-bubbled DMF and 4 mL of water. The solution was heated at 80 °C for 4 h. After cooling down, 250 mL of water was added. The solvents were partially evaporated on the rotary evaporator. The precipitated solid was collected by filtration, washed with water, and vacuum-dried. The obtained mixture was separated by column chromatography on silica gel with gradient elution from CH_2Cl_2 to 96:4 CH_2Cl_2/acetone mixture. **OxP(4NH$_2$Bn)$_3$** and **OxP(4NH$_2$Bn)$_4$** were isolated. Yield: 0.58 g (62 %). UV/Vis (CH_2Cl_2): λ_{max} (ε, M^{-1} cm^{-1}) = 249 (63800), 276 (42800), 328 (19700), 511 (148000) nm. ^{1}H NMR (400 MHz, $CDCl_3$): δ 7.24 (s, 8H), 6.64 (s, 8H), 6.39–6.46 (m, 16H), 4.34 (s, 8H), 3.57 (s, 8H), 1.25 (s, 72H) ppm. ^{13}C NMR (100.5 MHz, CDCl3): δ 186.1, 147.6, 146.1, 138.7, 133.4, 131.9, 131.6, 127.5, 127.4, 121.1, 114.9, 48.4, 35.5, 29.4 ppm. FTIR (ATR): ν = 3460 (br), 3358 (br), 3233 (br), 3001 (w), 2954 (s), 2913 (m), 2864 (m), 1665 (br), 1650 (w), 1640 (w), 1622 (m), 1589 (s, carbonyl C=O stretching), 1519 (s), 1489 (m), 1454 (m), 1407 (w), 1386 (w), 1376 (w), 1359 (s), 1333 (w), 1311 (br), 1256 (m), 1201 (w), 1177 (m), 1128 (w), 1089 (s), 1041 (m), 1016 (m), 957 (m), 945 (m), 928 (m), 906 (w), 888 (m), 865 (m), 838 (m), 820 (s), 809 (w), 788 (m), 741 (s), 715 (w), 661 (m), 638 (w), 623 (s) cm^{-1}. HRMS (ESI-TOF+): found: 1546.9537, calcd.: 1546.9584.

OxP(3,5Br$_2$Bn)$_4$

A round-bottom flask was charged with 5,10,15,20-tetrakis(3,5-di-tert-butyl-4-hydroxyphenyl)porphyrin (0.50 g, 0.45 mmol) and sodium hydride (108 mg, 2.7 mmol). Acetone (50 mL) was added and the mixture was stirred for 15 minutes. 3.5-Dibromobenzyl bromide (2.55 g, 11.5 mmol) dissolved in acetone (15 mL) was then added and the mixture was heated under reflux for 6 h. The reaction mixture was allowed to cool, the solvent was evaporated under reduced pressure and the product was isolated from the residue by column chromatography (SiO_2/CH_2Cl_2). Yield: 495 mg (52 %). UV/Vis (CH_2Cl_2): λ_{max} (ε, M^{-1} cm^{-1}) = 272 (26900), 325 (21300), 493 (137000) nm. ^{1}H NMR (400 MHz, $CDCl_3$): δ 7.47 (d, J = 1.6 Hz, 4H), 7.25, (s, 8H), 6.76 (d, J = 1.6 Hz, 8H), 6.73 (s, 8H), 4.35 (s, 8H), 1.28 (s, 72H) ppm. ^{13}C NMR (100.5 MHz, $CDCl_3$): δ 185.9, 149.4, 140.4, 137.3, 134.8, 134.1, 129.9, 128.2, 123.5, 120.6, 47.4, 35.7, 29.4 ppm. FTIR (ATR): ν = 3184 (w), 3118 (w), 2953 (s), 2914 (m), 2865 (m), 1639 (w), 1597 (s), 1558 (m), 1526 (m), 1488 (m), 1454 (m), 1425 (m), 1402 (w), 1388 (w), 1360 (s), 1323 (m), 1308 (s), 1257 (m), 1232 (w), 1221 (w), 1198 (m), 1087 (s), 1042 (m), 1017 (m), 992 (w), 654 (m), 930 (m), 919 (w), 886 (m), 855 (m), 839 (s), 813 (s), 799 (s), 753 (m), 734 (s), 716 (m), 704 (m), 692 (w), 674 (m), 664 (m), 626 (s), 608 (w) cm^{-1}. MALDI-TOF: found: 2116.376, calcd.: 2117.179.

OxP(F$_5$Bn)$_4$

A round-bottom flask was charged with **OxP** (0.83 g, 0.74 mmol), potassium carbonate (2.03 g, 14.7 mmol), and acetone (80 mL). Pentafluorobenzyl bromide (1.55 g, 5.9 mmol) dissolved in acetone (20 mL) was then added and the mixture was heated under reflux. After 2 h, another portion of potassium carbonate (2.03 g, 14.7 mmol) was added. After 20 h of refluxing, the reaction mixture was allowed to cool, the reaction mixture was filtered through a Büchner funnel and the filtrate was evaporated under reduced pressure. The solid residue was dissolved in CH_2Cl_2 (50 mL) and the insoluble part (mainly the dialkylated product) was filtered off. The product was isolated by column chromatography on SiO_2 eluting with CH_2Cl_2. Yield: 140 mg (10 %). UV/Vis (CH_2Cl_2): λ_{max} (ε, M^{-1} cm^{-1}) = 249 (63800), 276 (42800), 328 (19700), 490 (190000) nm. ^{1}H NMR (400 MHz, $CDCl_3$): δ 7.37 (s, 8H), 6.58 (s, 8H), 4.67 (s, 8H), 1.26 (s, 72H) ppm. ^{13}C NMR (100.5 MHz, $CDCl_3$): δ 186.0, 149.3, 137.6, 135.3, 130.2, 127.8, 120.7, 39.6, 35.7, 29.3 ppm. ^{19}F NMR (376.3 MHz, $CDCl_3$): δ -144.7 (d, J = 17.3, 2F), -151.9 (t, J = 21.8, 1F), -160.2 (t, J = 18.8, 2F) ppm. FTIR (ATR): ν = 3188 (w), 2957 (s), 2913 (m), 2867 (m), 1656 (w), 1642 (w), 1601 (s), 1522 (s), 1501 (s), 1456 (w), 1426 (w), 1405 (w), 1380 (w), 1361 (s), 1333 (m), 1318 (s), 1303 (m), 1255 (m), 1229 (w), 1200 (w), 1176 (w), 1140 (w), 1121 (s), 1088 (m), 1043 (m), 1001 (s), 946 (s), 931 (m), 906 (m), 887 (w), 879 (w), 863 (m), 838 (w), 820 (m), 807 (m), 793 (s), 743 (w), 722 (s), 688 (w), 676 (w), 661 (m), 626 (s), 602 cm^{-1}. HRMS (ESI-TOF+): found: 2119.1855, calcd.: 2119.1940.

OxP(4TPABn)$_4$

A round-bottom flask was charged with **OxP(4BrBn)$_4$** (700 mg, 0.39 mmol), $PdCl_2$(dppf)·CH_2Cl_2 (637 mg, 0.78 mmol), 4-(N,N-diphenylamino)phenylboronic acid (1.12 g, 3.87 mmol) and K_2CO_3 (259 mg, 1.87 mmol). The flask was purged three times with N_2. The reactants were dissolved in a degassed mixture of 1,4-dioxane/water (6:1 v/v). The reaction mixture was heated under N_2 at 100 °C for 24 h. After allowing the reaction to cool to room temperature, solvents were removed by rotary evaporation, then the solid residue was dissolved in CH_2Cl_2 and filtered. The solvent was evaporated from the resulting filtrate under reduced pressure and the product was isolated by column chromatography (SiO_2/CH_2Cl_2) and recrystallized from CH_2Cl_2/hexane mixture. Yield: 520 mg (54 %). UV/Vis (CH_2Cl_2): λ_{max} (ε, M^{-1} cm^{-1}) = 334 (121000), 505 (149000) nm. ^{1}H NMR (400 MHz, $CDCl_3$): δ 7.35 (d, J = 8.0 Hz, 8H), 7.31–7.22 (m, 32H), 7.09–7.00 (m, 32H), 6.74–6.72 (m, 16H), 4.58 (s, 8H), 1.22 (s, 72H) ppm. ^{13}C NMR (100.5 MHz, $CDCl_3$): δ 186.0, 148.0, 147.7, 147.6, 140.6, 138.7, 136.0, 133.9, 133.6, 131.6, 130.7, 129.4, 127.6, 126.9, 126.6, 124.6, 123.7, 123.2, 121.2, 48.6, 35.5, 29.4 ppm. FTIR (ATR): ν = 3182 (w), 3061 (w), 3032 (w), 2999 (w), 2953 (s), 2912 (m), 2883 (w), 2864 (m), 1591 (s), 1525 (m), 1487 (s), 1454 (m), 1404 (w), 1387 (w), 1373 (w), 1360 (s), 1323 (w), 1311 (s), 1290 (w), 1273 (s), 1257 (s), 1194 (w), 1178 (w), 1155 (w), 1115 (w), 1088 (m), 1039 (m), 1016 (m), 1005 (w), 957 (m), 949 (w), 928 (m), 920 (w), 906 (w), 887 (m), 864 (m), 835 (m), 818 (w), 806 (s), 791 (m), 750 (s), 731 (w), 717 (w), 692 (s), 681 (w), 661 (m), 644 (w), 634 (w), 621 (s) cm^{-1}. HRMS (ESI-TOF+): found: 2458.3240 ($[M + H]^+$), calcd.: 2458.3261.

OxP(4MeOTPABn)$_4$

A round-bottom flask was charged with **OxP(4BrBn)$_4$** (250 mg, 0.14 mmol), $PdCl_2$(dppf)·CH_2Cl_2 (225 mg, 0.28 mmol), 4-(N,N-bis(4-methoxyphenyl)amino)phenylboronic acid (485 mg, 1.39 mmol) and K_2CO_3 (93 mg, 0.67 mmol). The flask was purged three times with N_2. The reactants were dissolved in a degassed mixture of 1,4-dioxane/water (6:1 v/v). The reaction mixture was heated under N_2 at 100 °C for 24 h. After allowing the reaction to cool to room temperature, solvents were

removed by rotary evaporation, then the solid residue was dissolved in CH_2Cl_2 and filtered. The solvent was evaporated from the resulting filtrate under reduced pressure and the product was isolated by column chromatography (SiO_2/CH_2Cl_2) and recrystallized from CH_2Cl_2/hexane mixture. Yield: 94 mg (25 %). UV/Vis (CH_2Cl_2): λ_{max} (ε, M^{-1} cm^{-1}) = 336 (113000), 505 (143000) nm. ^{1}H NMR (400 MHz, $CDCl_3$): δ 7.32 (d, J = 8.4 Hz, 8H), 7.29 (s, 8H), 7.23 (d, J = 8.0 Hz, 8H), 7.04 (d, J = 9.2 Hz, 16H), 6.90 (d, J = 8.4 Hz, 8H), 6.81 (d, J = 9.2 Hz, 16H), 6.72 (s, 8H), 6.70 (d, J = 8.0 Hz, 8H), 4.56 (s, 8H), 3.78 (s, 24H), 1.22 (s, 72H) ppm. ^{13}C NMR (100.5 MHz, $CDCl_3$): δ 186.0, 156.1, 148.6, 148.0, 140.7, 138.6, 135.6, 133.9, 131.6, 130.8, 127.4, 126.8, 126.7, 126.5, 121.1, 120.5, 114.8, 55.6, 35.5, 29.4 ppm. FTIR (ATR): ν = 3178 (w), 3110 (w), 3101 (w), 3035 (w), 2997 (w), 2953 (s), 2906 (m), 2866 (w), 2833 (m), 1639 (w), 1593 (s), 1527 (m), 1495 (s), 1454 (m), 1441 (w), 1404 (w), 1387 (w), 1371 (w), 1360 (s), 1313 (s), 1282 (w), 1238 (s), 1194 (w), 1178 (m), 1167 (w), 1105 (w), 1088 (m), 1036 (s), 1016 (m), 957 (m), 947 (w), 930 (w), 922 (w), 906 (w), 887 (w), 864 (w), 825 (s), 808 (s), 756 (m), 744 (w), 719 (m), 669 (w), 640 (w), 623 (m) cm^{-1}. HRMS (ESI-TOF+): found: 1348.7023 ($[M]^{2+}$), calcd.: 1348.7011.

RESULTS AND DISCUSSION

The chemical structures of the **OxP** derivatives used in this work are shown in Chart 1. **OxP** can be substituted with different groups by N-substitution at pyrrole nitrogen atoms and/or modifications at the pyrrole β-position, although the latter is limited here to persubstitution with bromine. Variation of multiplicity and identity of N-substituent on **OxP** was investigated for its effect on the efficiency of $^1O_2$ generation in solution. The effect of β-perbromination and N-substituent multiplicity of **OxP** was assessed only for the 4-bromobenzyl substituent (Chart 1). In this case, for a direct comparison of quantum yields of $^1O_2$ generation of the compounds studied, we have selected toluene as the solvent for this study due to the excellent solubility of all the compounds in that solvent (**Br_8OxP** compounds exhibit only limited solubility in chlorinated solvents and toluene has been used also to avoid any effects due aggregation). For this reason, we have selected C_{60} fullerene as a reference material for the determination of relative $^1O_2$ quantum yield due to its suitable solubility in toluene and unity $^1O_2$ quantum yield (Φ_Δ = 1) at all points where it absorbs in its electronic absorption spectrum.[43,44]

<**Chart 1**>

X-ray crystal structures of several of the compounds are available from previous works and are shown in Fig. 1. N-substitution of **OxP** occurs without altering the saddle geometry with double N-substitution at N_{21}, N_{23} occurring on the same face of the molecule and tetra-N-substitution at alternating faces for N_{21}, N_{22}, N_{23} and N_{24}, as shown in Fig. 2. A key parameter in discussing the structures of these compounds is the dihedral angle subtended between the macrocyclic average plane and the planes of the pyrrole rings, which is 48° for all pyrrole rings in **OxP** (Fig. 1a). N-substitution increases this angle to around 65° in **$OxPBn_2$** for the N-benzyl pyrrole groups (Fig 1b). Buckling of the macrocycle upon per-N-substitution apparently allows a reduction in the corresponding angle in **$OxPBn_4$** to 53° (Fig. 1c), although crystal packing forces probably affect macrocyclic puckering since the $(4BrBn)_4$ derivative (Fig. 1d) exhibits a less distorted structure. Per-β-bromination increases the angle subtended by the N-benzyl groups in **β-Br_8OxP(4BrBn)$_2$** to 72° and in **β-Br_8OxP(4BrBn)$_4$** to 65°, which is responsible for the blue shift in the absorption maxima of these compounds.

<**Fig. 1**>

For compounds that have not been studied X-ray crystallographically, selected energy-minimized structures are shown in Fig. 2. **OxP(3,5Br$_2$Bn)$_4$** (Fig 2a), **OxP(F$_5$Bn)$_4$** (Fig. 2b) and **OxP(4TPABn)$_4$** (Fig. 2c) are elaborated at the N-benzyl substituents without substantially changing the form of the **OxPBn$_4$** unit.

<**Fig. 2**>

Electronic absorption (UV-vis) spectra of selected compounds are shown in Fig. 3. Fig. 3a shows UV-vis spectra of **OxP**, **OxP(4BrBn)$_2$** and **OxP(4BrBn)$_4$** indicating the absorption maximum around 500 nm (general for most simple **OxP** compounds). **OxP** has an absorption maximum at 518 nm with a tail which extends across the visible range into the near infrared region. The broadness of its spectrum has been attributed to delocalization and tautomeric processes,[1] which are obstructed in the N-alkylated derivatives **OxP(4BrBn)$_2$** and **OxP(4BrBn)$_4$** leading to a narrowing of the absorption band around 510 nm and a small hypsochromic shift (to 504 nm for **OxP(4BrBn)$_4$**). Bromination of the **OxP** macrocyclic beta positions leads to more substantial hypsochromic shifts (~30 nm) in the absorption maxima of **β-Br$_8$OxP** (to 487 nm), **β-Br$_8$OxP(4BrBn)$_2$** (509 to 487 nm) and **Br$_8$OxP(4BrBn)$_4$** (504 to 472 nm), which is due to increased macrocyclic puckered and a reduction in electronic conjugation (see Fig. 3b). Thus, bromination has a similar effect to N-alkylation presumably because both these modifications lead to reductions in conformational flexibility of the tetrapyrrole core and increased macrocycle distortion. Notably, **β-Br$_8$OxP** has no absorption tail into the near infrared region and its N-alkylation leads only to small hypsochromic shifts in the **OxP** absorption maximum (Fig. 3b). In tetra-N-alkylated derivatives of **OxP** (see Fig. 3c), the presence of electron-withdrawing or electron-accepting groups appears to lead to weak bathochromic or hypsochromic shifts of the absorption maximum, respectively. For example, **OxPBn$_4$(4NO$_2$Bn)$_4$** shifts the maximum by 14 nm to 485 nm while **OxPBn$_4$(4NH$_2$Bn)$_4$** shifts it by 8 nm to 506 nm. In the spectrum of **OxP(4TPABn)$_4$** (green line in Fig. 3c), the large absorption around 320 nm is characteristic of the triphenylamine chromophore.

<**Fig. 3**>

Quantum yields of $^1O_2$ generation (Φ_Δ) were estimated by measuring the intensity of $^1O_2$ photoluminescence from solutions of the compounds under irradiation relative to that of C_{60} in toluene. We have considered the effects of (a) N-substituent multiplicity, (b) β-perbromination/N-substituent multiplicity, and (c) N-substituent identity in **OxPBn$_4$** type compounds.

<**Fig. 4**>

<**Table 1**>

Fig. 4 shows spectroscopic data obtained from compounds of different N-substituent multiplicities, i.e., 0, 2 or 4 4-bromobenzyl groups. Fig. 4a shows absorption spectra of the sample solutions normalized at the corresponding irradiation wavelength (510 nm) used for $^1O_2$ generation. Fig. 4b shows $^1O_2$ photoluminescence spectra of the same solutions under irradiation indicating that N-substitution increases the relative $^1O_2$ yield in the order **OxP** < **OxP(4BrBn)$_2$** < **OxP(4BrBn)$_4$**. This data reveals a substantial increase in yield for the tetra-N-substituted compound. Non-N-substituted **OxP** appears to generate $^1O_2$ only weakly. The weak $^1O_2$ generating activity observed here for **OxP** is probably actually due to the presence

of the corresponding free base porphyrin **TDtBHPP**, which has a modest absorbance in the visible range around 520 nm. The fluorescence spectrum of the solution containing **OxP** (Fig. 4c) contains peaks around 650 and 720 nm, which are characteristic of the presence of the corresponding free base porphyrin. **OxP** is unstable against reduction in solution and samples left standing to acquire a significant porphyrin content even in the solid state. This may be due to photo-induced water oxidation reaction and, in this case, can be promoted by irradiation of the **OxP** solution.[1] N-alkylation of OxP prevents reduction processes back to the porphyrin so that fluorescence spectra of **OxP(4BrBn)$_2$** and **OxP(4BrBn)$_4$** contain contributions only from the **OxP** chromophore. Quantum yields of singlet oxygen generation of the compounds are shown in Table 1. **OxP(4BrBn)$_4$** has a large Φ_Δ of 0.75, which is competitive with other chromophores used in the relevant applications of PDT and bacterial inactivation.

<**Fig. 5**>

<**Table 2**>

In previous work, we have also reported the synthesis, isolation and structures of N-alkylated per-β-brominated **OxP** derivatives **β-Br$_8$OxP**, **β-Br$_8$OxP(4BrBn)$_2$**[41] and **β-Br$_8$OxP(4BrBn)$_4$**.[42] Fig. 5 shows spectroscopic data relevant to the $^1O_2$ generation properties of these compounds. Fig. 5a shows the absorption spectra of the compounds normalized at the irradiation wavelength (500 nm). β-Octabromination leads to a blue shift of ~25-30 nm in the **OxP** absorption maximum due to inductive effects due to the bromo-substituents.[41] Fig. 5b shows the $^1O_2$ response at 1275 nm and again indicates an increase in quantum yield on increasing N-alkylation. **Br$_8$OxP** exhibits a high Φ_Δ compared to **OxP** while N-alkylation nearly doubles this value for both of the N-alkylates (see Table 2). Interestingly, the fluorescence emission from the compounds is effectively quenched by increasing N-alkylation, which could be an effect of the increasing $^1O_2$ quantum yield being exhibited as a decrease in emission intensity due to the change in the mode of excitation energy loss from radiative towards the energy transfer to atmospheric oxygen via the triplet excited state. These data indicate that **Br$_8$OxP** derivatives, even the parent compound, are capable of generating singlet oxygen at a useful level.

<**Fig. 6**>

<**Table 3**>

Based on data obtained for the **OxP** and **Br$_8$OxP** families of compounds, it appears that the tetra-N-alkylated **OxP** compounds represent the optimized form of the chromophore for $^1O_2$ generation. Therefore, we have studied the available tetra-N-benzylated compounds. Fig. 6 shows spectroscopic data used to estimate the Φ_Δ values of these compounds. Φ_Δ data is summarized in Table 3 where compounds are listed according to their increasing Φ_Δ values. Several observations can be made about the data including that electron-donating groups such as amino or 4-methoxyTPA are detrimental to the value of Φ_Δ while electron-withdrawing groups are present in compounds with larger Φ_Δ. A well-known method to improve Φ_Δ of $^1O_2$ generating chromophores is to replace hydrogen atoms bonded to the chromophore with heavy atoms such as bromine or iodine (the so-called heavy atom effect).[45] In this case, this effect does not hold well for the per-β-brominated **OxP** derivatives **β-Br$_8$OxP**, **β-Br$_8$OxP(4BrBn)$_2$** and **β-Br$_8$OxP(4BrBn)$_4$** although modest improvements in Φ_Δ were found. The effect is most pronounced for compounds with increasingly high halogen substitution culminating in the perfluorobenzyl derivative **OxP(F$_5$Bn)$_4$**.

It is presently unclear whether the non-N-substituted OxP chromophore is capable of photosensitizing singlet oxygen. Its poor or lack of activity might be due to the availability of other routes of relaxation by conformational variation of the saddle macrocycle or even tautomeric processes.[1,17] This is supported circumstantially by the structure of the **β-Br$_8$OxP** derivative where multiple β-bromine atoms obstruct macrocyclic processes, rigidifying the chromophore. While **β-Br$_8$OxP** is likely of lower macrocyclic flexibility, it still contains multiple NH groups, which appear detrimental to $^1O_2$ generation in **OxP** derivatives based on the data in Tables 1 & 2. However, it is not possible easily to separate these effects from other heavy atom effects due to the presence of multiple Br atoms. The most important feature to note is that **β-Br$_8$OxP(4BrBn)$_4$** has an Φ_Δ inferior to the non-Br derivative suggesting that perbromination at the tetrapyrrole macrocycle is not beneficial for $^1O_2$ generation in the optimal tetra-N-substituted **OxPBn$_4$** compounds. In those compounds, it is possible to consider the effects of N-benzyl substituent substituents, including those of electron-donating vs electron withdrawing and multiplicity of halogen atoms. Basically, free amine groups have a strong negative effect on Φ_Δ while other groups having electron-donating groups are also not favored. This is most likely due to photo-induced electron transfer between electron rich N-substituents and electron deficient OxP chromophore, which is known to be a significant property in similar compounds,[13,14,20] and results in quenching of the excited states required for singlet oxygen generation. Multiple halogen atom substitution at the N-benzyl group (as opposed to β-substitution) leads to the highest so far observed values of Φ_Δ for **OxP** compounds. Finally, **OxPBn$_4$(4NO$_2$Bn)$_4$** and **OxPBn$_4$(4CO$_2$MeBn)$_4$** also exhibit Φ_Δ values around 0.75 indicating that electron-withdrawing groups can also promote the efficiency of $^1O_2$ photosensitization in N-substituted **OxP** compounds.

OxPBn$_4$ has only recently emerged as an effective $^1O_2$ photosensitizer. It is an important addition to this class of compounds because of its synthetic flexibility, strong absorption in the visible region (see Fig. 6c) and high stability under irradiation (see Fig. 6d). The **OxPBn$_4$** class of compounds is complementary to the existing compound types such as *meso*-tetraphenylporphyrins/chlorins (TPP,[46] TPC[47]), Rose Bengal derivatives,[37] phenalenones[38] fuchsonarenes,[48] and fullerenes,[36] amongst others.[49,50] Each of these families of compounds has its own benefits and also disadvantages. For instance, $^1O_2$ photosensitizer activity of porphyrins can be quenched due to aggregation in particular media while fullerene derivatives can also suffer the effects of aggregation or poor solubility, as well as being deactivated for $^1O_2$ generation in aqueous media due for various reasons. Molecular design of appropriate **OxPBn$_4$** derivatives can be used to eliminate these disadvantages in the corresponding compounds providing a useful alternative to the existing materials. Whilst the extinction coefficients of **OxP** derivatives are typically lower than porphyrins, their broad absorption profiles over a large section of the visible region means that a broader range of excitation sources can be used. They also offer the potential for a larger photon absorption density and comparable stabilities to the currently used classes of chromophores. The non-planarity of the **OxP** system gives access to 3-dimensional scaffolds that are not traditionally obtainable utilizing planar chromophores, which have already proven useful in the preparation of porous coordination polymers.[15] Finally, in this work we have identified several key features of **OxP** derivatives important for optimizing their singlet oxygen generating capabilities. This has also revealed some unusual features of the compounds including certain perhaps counterintuitive properties. These include the fact of the property optimization based on variation in structure of non-conjugated N-benzyl substituents, and fluorescence quenching according to increasing N-substitution in the **β-Br$_8$OxP** series. For the former, it is likely that the sterically crowded nature of the **OxPBn$_4$** derivatives promotes the influence even of non-conjugated N-substituents either by inductive or through space effects. Fluorescence quenching according to increasing N-substitution in the **β-Br$_8$OxP**

series is more difficult to account for but might be due to reductions in conjugative overlap between moieties of the **OxP** chromophore resulting in inaccessible excited states.

CONCLUSIONS

To summarize, we have established some of the design rules to optimize the molecular structures of $^1O_2$ photosensitizers based on the **OxP** chromophore. These are: (1) tetra-N-substitution is the optimal form of **OxP** compound; (2) bromination of the **OxP** chromophore improves Φ_Δ but not in the **OxPBn$_4$** compounds; (3) electron-withdrawing groups (nitro, ester) on the N-benzyl groups promote Φ_Δ; (4) increased multiplicity of halogen substitution at the N-benzyl substituents optimizes Φ_Δ with perfluorobenzyl groups so far providing the best characteristics, **OxP(F$_5$Bn)$_4$**. The synthetic possibilities of the **OxP** system suggest developments of materials for this application in various directions, and we will report advances in the preparation of **OxP**-based $^1O_2$ photosensitizers in due course. In particular, the addition of water-solubilizing groups such as ethylene glycol chains might provide materials for use in aqueous systems similar to that found for TPP-type compounds.[51]

Acknowledgements

D.T.P is grateful to the National Institute for Materials Science, International Center for Young Scientists, Japan (ICYS, NIMS) for an ICYS fellowship and research funds. J.H. is grateful to the Japan Society for the Promotion of Science (JSPS) for a JSPS Fellowship. FD is grateful for support by the US National Science Foundation. This research was partly supported by World Premier International Research Center Initiative (WPI Initiative), MEXT, Japan.

REFERENCES

1. Milgrom LR. *Tetrahedron* 1983; **39**: 3895–3898.
2. Milgrom LR, Flitter WD, Short EL. *J. Chem. Soc., Chem. Commun.* 1991; 788–790.
3. Milgrom LR, Flitter WD. *Tetrahedron* 1992; **48**: 2951–2956.
4. Evans TA, Srivatsa GS, Sawyer, DT, Traylor TG. *Inorg. Chem.* 1985; **24**: 4733–4735.
5. Traylor TG, Nolan KB, Hildreth R, Evans TA. *J. Am. Chem. Soc.* 1983; **105**: 6149–6151.
6. Hill JP, Hewitt IJ, Anson CE, Powell AK, McCarty AL, Karr PA, Zandler ME, D'Souza F. *J. Org. Chem.* 2004; **69**: 5861–5869.
7. Hill JP, Schmitt W, McCarty AL, Ariga K, D'Souza F. *Eur. J. Org. Chem.* 2005; 2893–2902.
8. Golder AJ, Milgrom LR, Nolan KB, Povey DC. *J. Chem. Soc., Chem. Commun.* 1989; 1751–1753.
9. Milgrom LR, Hill JP, Dempsey PF. *Tetrahedron*, 1994; **50**: 13477–13484.
10. Ishihara S, Hill JP, Shundo A, Ohkubo K, Fukuzumi S, Elsegood MRJ, Teat SJ Ariga K. *J. Am. Chem. Soc.* 2011; **133**: 16119–16126.
11. Chahal MK, Sankar M. *Dalton Trans.* 2018; **45**: 16404–16412.
12. Cong L, Chahal MK, Osterloh R, Sankar M, Kadish KM. *Inorg. Chem.* 2019; **58**: 14361–14376.
13. Hill JP, Sandanayaka ASD, McCarty AL, Karr PA, Zandler ME, Charvet R, Ariga K, Araki Y, Ito O, D'Souza F. *Eur. J. Org. Chem.* 2006; 595–603.
14. Schumacher AL, Sandanayaka ASD, Hill JP, Ariga K, Karr PA, Araki Y, Ito O, D'Souza F. *Chem. Eur. J.* 2007; **13**: 4628–4635.

15. Hynek J, Payne DT, Chahal MK, Sciortino F, Matsushita Y, Shrestha LK, Ariga K, Labuta J, Yamauchi Y, Hill JP. *Mater. Today. Chem.* 2021; **21**: 100534.
16. Labuta J, Hill JP, Elsegood MRJ, Ariga K. *Tetrahedron Lett.* 2010; **51**: 2935–2938.
17. Xie Y, Hill JP, Schumacher AL, Karr PA, D'Souza F, Anson CE, Powell AK, Ariga K. *Chem. Eur. J.* 2007; **13**: 9824–9833.
18. Hill JP, Schumacher AL, D'Souza F, Labuta J, Redshaw C, Elsegood MJR, Aoyagi M, Nakanishi T, Ariga K. *Inorg. Chem.* 2006; **45**: 8288–8296.
19. Labuta J, Ishihara S, Šikorský T, Futera Z, Shundo A, Hanyková L, Burda JV, Ariga K and Hill JP. *Nat. Commun.* 2013; **4**: 2188.
20. D'Souza F, Subbaiyan NK, Xie Y, Hill JP, Ariga K, Ohkubo K, Fukuzumi S. *J. Am. Chem. Soc.* 2009; **131**: 16138–16146.
21. Geng F, Gao H, Meng O, Dong Z, Wakayama Y, Akada M, Ariga K, Hill JP. *Chem. Commun*. 2011; **47**: 8533–8535.
22. Kashyap A, Ramasamy E, Ramalingam V, Pattabiraman M. *Molecules* 2021; **26**: 2673.
23. Li X, Kolemen S, Yoon J, Akkaya, EU. *Adv. Funct. Mater.* 2007; **27**: 1604053.
24. Ghogare AA, Greer A. *Chem. Rev.* 2016; **116**: 9994–10034.
25. Pibiri I, Buscemi S, Picciolello, AP, Pace A. *ChemPhotoChem* 2018; **2**: 535–547.
26. Garcia-Fresnadillo D. *ChemPhotoChem* 2018; **2**: 512–534.
27. Benov L. *Med. Princ. Pract.* 2015; **24** (Suppl 1): 14–28.
28. Vera C, Tulli F, Borsarelli CD. *Front. Bioeng. Biotechnol.* 2021; **9**: 655370.
29. Gunaydin G, Gedik EM, Ayan S. *Front. Chem.* (Lausanne, Switz.) 2021; **9**: 691697.
30. Lo PC, Rodriguez-Morgade MS, Pandey RK, Ng DKP, Torres T, Dumoulin F. *Chem Soc. Rev.* 2020; **49**: 1041–1056.
31. Halaskova M, Kostelansky F, Demuth J, Hlbocanova I, Miletin M, Zimcik P, Machacek M, Novakova V. *ChemPlusChem* 2022; **87**: e202200133.
32. Hynek J, Chahal MK, Payne DT, Labuta J, Hill JP. *Coord. Chem. Rev.* 2020; **425**: 213541.
33. Kruk M, Karotki A, Drobizhev M, Kuzmitsky V, Gael V, Rebane A. *J. Luminescence* 2003; **105**: 45–55.
34. Kumar S, Acharyya JN, Banerjee D, Soma VR, Prakash GV, Sankar M. *Dalton Trans.* 2021; **50**: 6256–6272.
35. Nonell S, Flors C. *Singlet Oxygen Applications in Biosciences and Nanosciences*, vol. 2. chapter 25. Royal Society of Chemistry: Cambridge, UK, 2016; p 9–26.
36. Arbogast JW, Darmanyan AP, Foote CS, Rubin Y, Diederich FN, Alvarez MM, Anz SJ, Whetten RL. *J. Phys. Chem.* 1991; **95**: 11–12.
37. Murasecco-Suardi P, Gassmann E, Braun AM, Oliveros E. *Helv. Chim. Acta* 1987; **70**: 1760–1773.
38. Schmidt R, Tanielian C, Dunsbach R, Wolff C. *J. Photochem. Photobiol. A: Chem.* 1994; **79**: 11–17.
39. Garcia-Fresnadillo D, Georgiadou V, Orellana G, Braun AM, Oliveros, E. *Helv. Chim. Acta* 1996; **79**: 1222–1238.
40. Xie Y, Hill JP, Schumacher AL, Sandanayaka ASD, Araki Y, Karr PA, Labuta J, D'Souza F, Ito O, Anson CE, Powell AK, Ariga K. *J. Phys. Chem. C* 2008; **112**: 10559–10572.
41. Webre WA, Hill JP, Matsushita Y, Karr PA, Ariga K, D'Souza F. *Dalton Trans.* 2016: **45**: 4006–4016.
42. Commins PJ, Hill JP, Matsushita Y, Webre WA, Labuta J, Ariga K, D'Souza F. *J. Porphyrins and Phthalocyanines* 2016; **20**: 213–222.
43. Wilkinson F, Helman WP, Ross AB. *J. Phys. Chem. Ref. Data* 1993; **22**: 113-262.

44. Prat F, Stackow R, Bernstein R, Qian W, Rubin Y, Foote CS. *J. Phys. Chem. A* 1999; **103**: 7230-7235.
45. Marian CM. *Ann. Rev. Phys. Chem.* 2021; **72**: 617–640.
46. Mosinger J, Mička Z. *J. Photochem. Photobiol. A: Chem.* 1997; **107**: 77–82.
47. Silva EFF, Schaberle FA, Monteiro CJP, Dabrowski JM, Arnaut LG. *Photochem. Photobiol. Sci.* 2013; **12**: 1187–1192.
48. Payne DT, Wenre WA, Gobeze HB, Seetharaman S, Matsushita Y, Karr PA, Chahal MK, Labuta J, Jevasuwan W, Fukata N, Fossey JS, Ariga K, D'Souza F, Hill JP. *Chem. Sci.* 2020; **11**: 2614–2620.
49. Lamberts JJM, Schumacher DR, Neckers DC. *J. Am. Chem. Soc.* 1984; **106**: 5879–5883.
50. Godard J, Brégier F, Arnoux P, Myrzakhmetov B, Champavier Y, Frochot C, Sol V. *ACS Omega* 2020; **5**: 28264–28272.
51. Payne DT, Hynek J, Labuta J, Hill JP. *Phys. Chem. Chem. Phys*. 2022; **24**: 6146–6154.

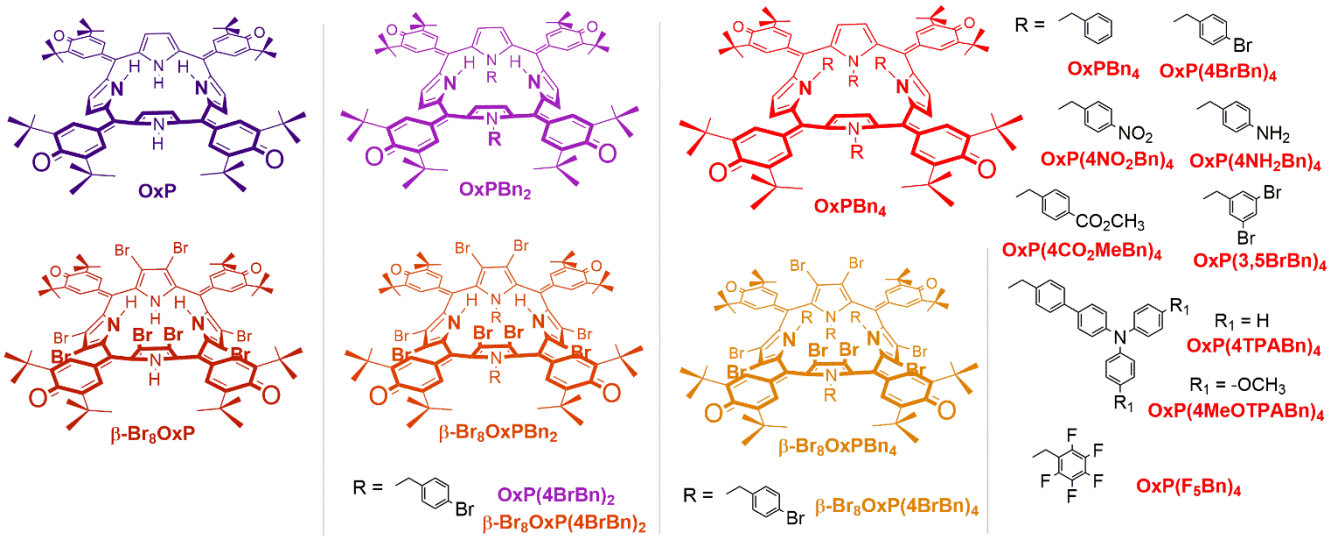

Chart 1. Chemical structures of the compounds studied in this work. Colors of the structures reflect the approximate hues of solutions of the relevant compounds in chlorinated solvents (non-N-substituted-**OxP**: dark purple; di-N-substituted-**OxP**: mauve; tetra-N-substituted-**OxP**: red, etc.). Abbreviations of the compounds are given for ease of reference in the text.

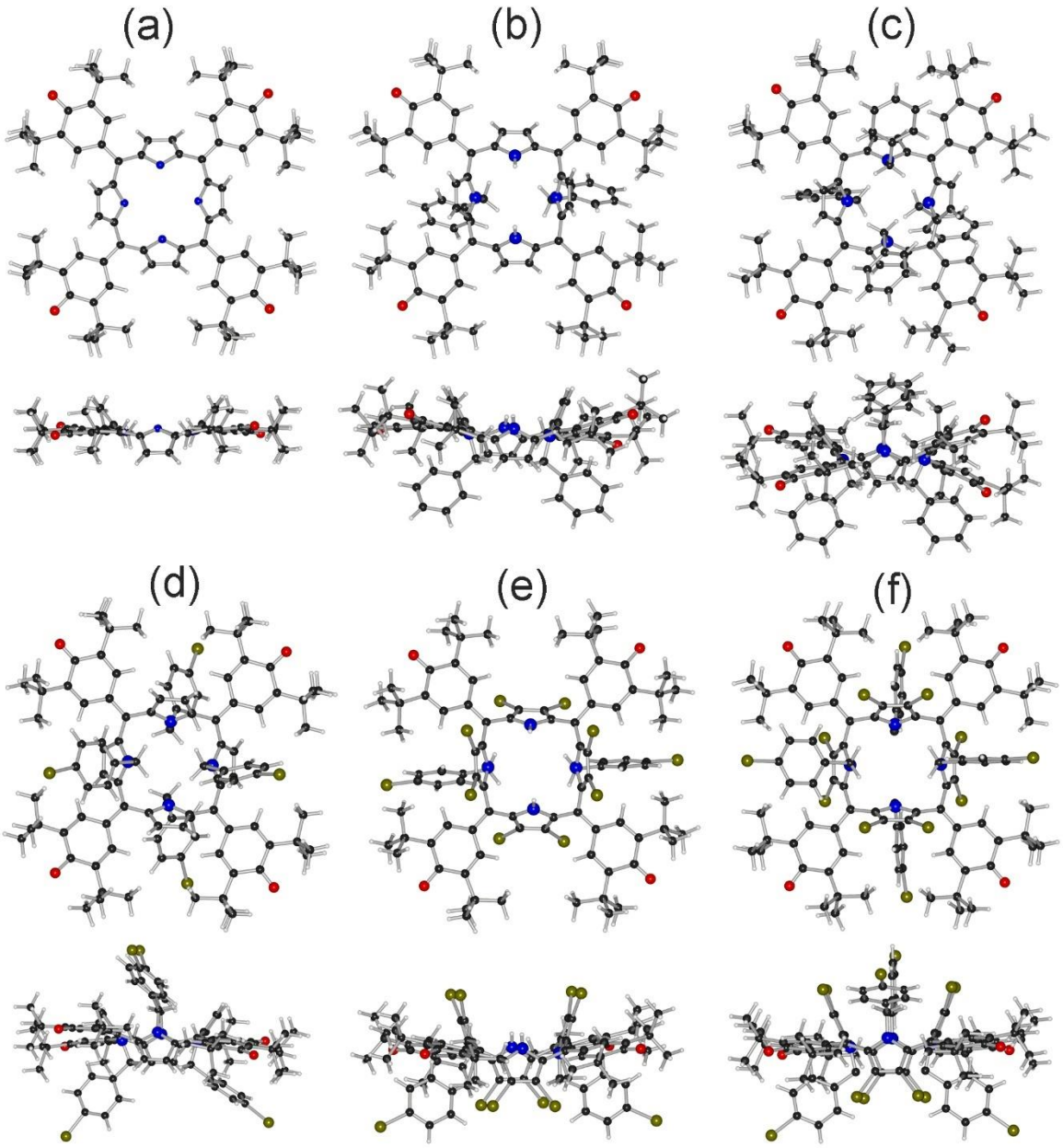

Fig. 1. Single crystal X-ray structures of (a) **OxP**,[8] (b) **OxPBn$_2$**,[6] (c) **OxPBn$_4$**,[6] (d) **OxP(4BrBn)$_4$**,[40] (e) **β-Br$_8$OxP(4BrBn)$_2$**,[41] (f) **β-Br$_8$OxP(4BrBn)$_4$**.[42]

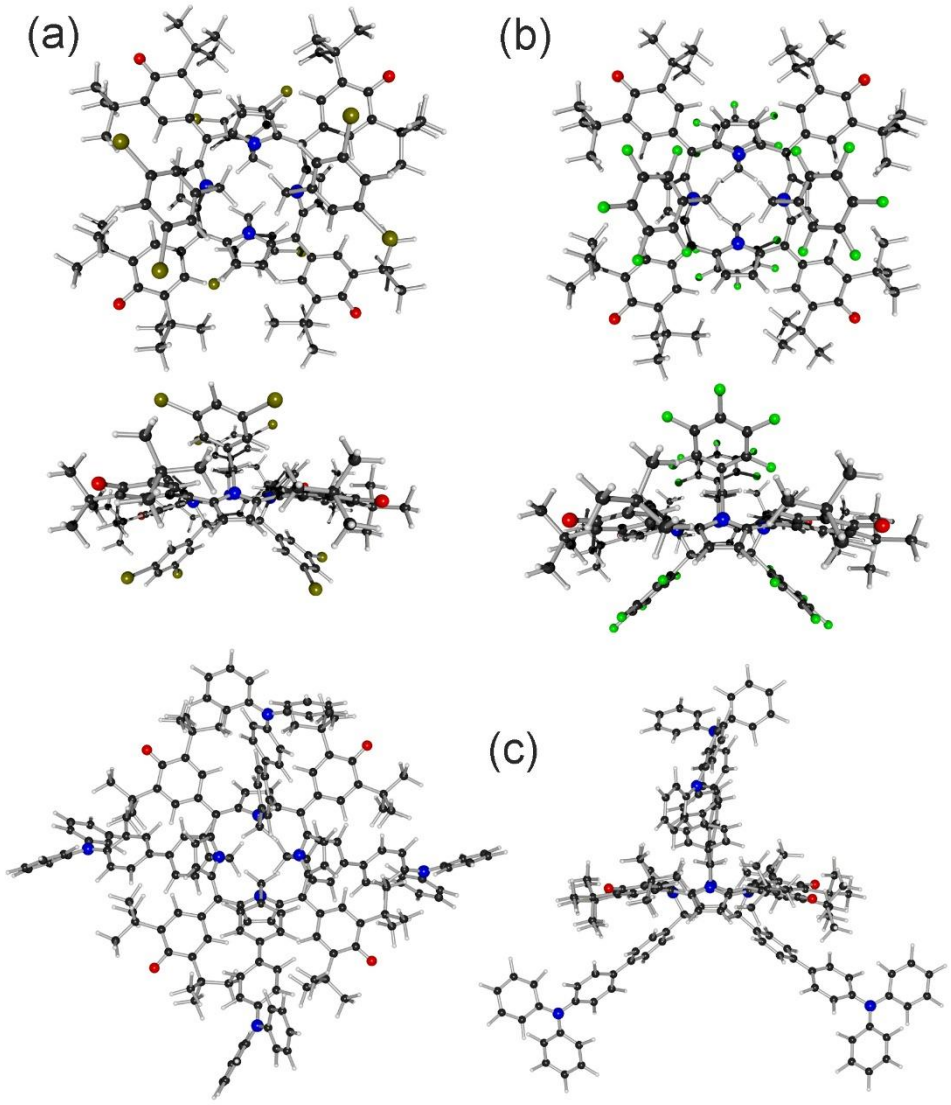

Fig. 2. Structures of (a) **OxP(3,5Br$_2$Bn)$_4$**, (b) **OxP(F$_5$Bn)$_4$**, (c) **OxP(4TPABn)$_4$** computed at the MM2 level using the ChemDraw3D program.

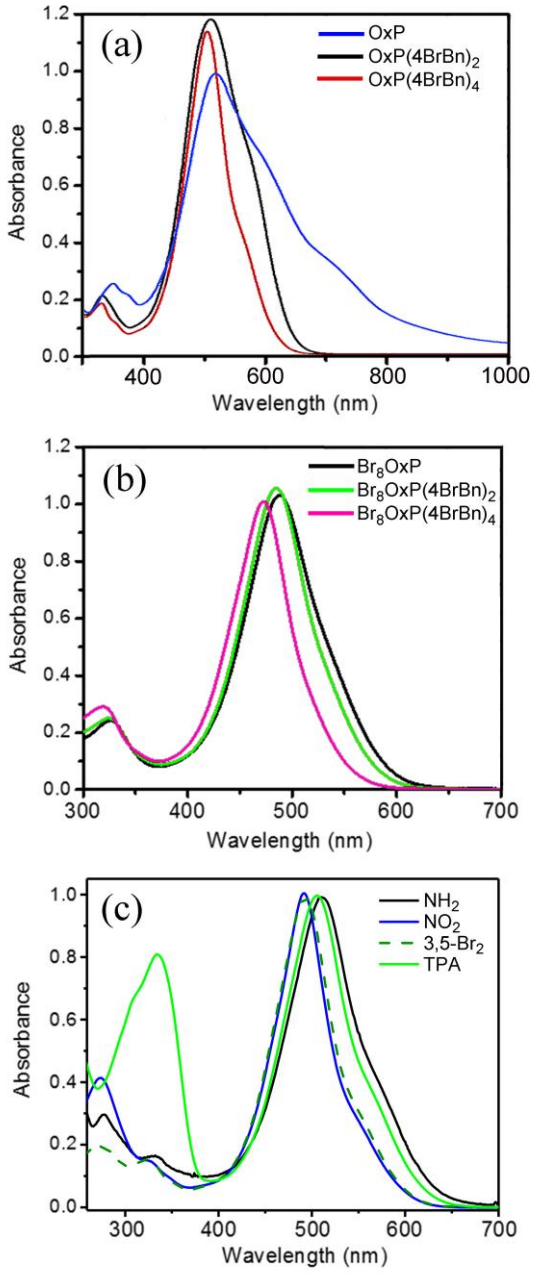

Fig. 3. Electronic absorption spectra of selected **OxP** compounds. (a) **OxP** (blue line), **OxP(4BrBn)$_2$** (black line) and **OxP(4BrBn)$_4$** (red line). (b) **β-Br$_8$OxP** (black line), **β-Br$_8$OxP(4BrBn)$_2$** (light green line) and **β-Br$_8$OxP(4BrBn)$_4$** (pink line). (c) **OxP(4NH$_2$Bn)$_4$** (black line), **OxP(4NO$_2$Bn)$_4$** (blue line), **OxP(3,5Br$_2$Bn)$_4$** (dark green dashed line) and **OxP(4TPABn)$_4$** (light green line).

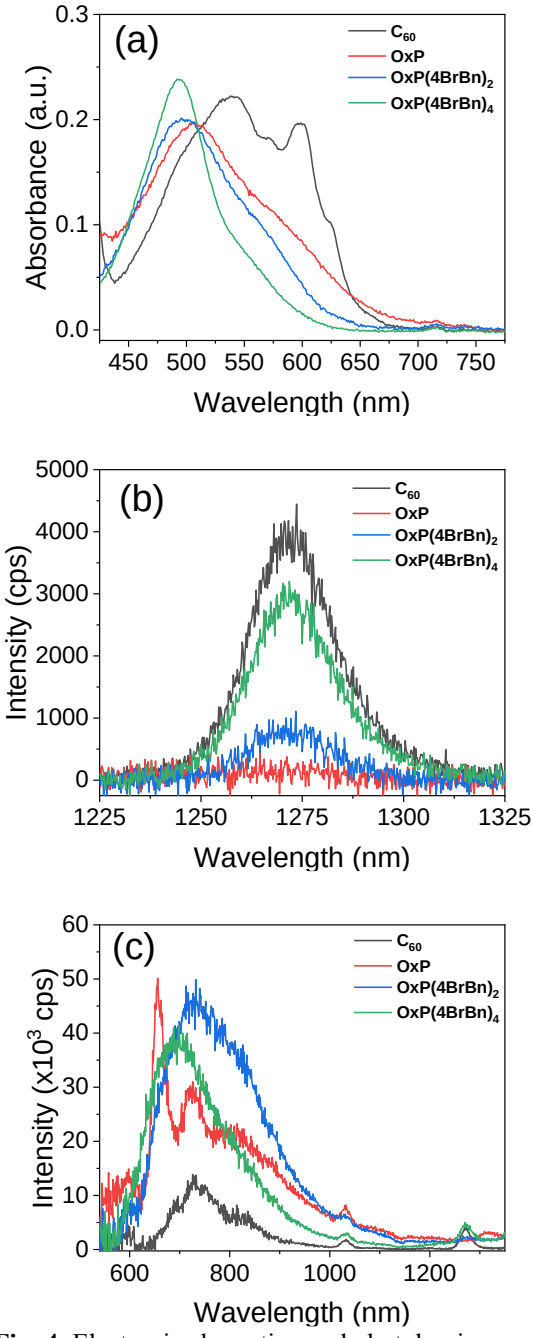

Fig. 4. Electronic absorption and photoluminescence spectra for **OxP**, **OxP(4BrBn)$_2$** and **OxP(4BrBn)$_4$**. (a) UV-vis spectra of solutions of the compounds and reference (C_{60}) having approximately equivalent absorbances at the wavelength of irradiation (510 nm) in toluene. (b) $^1O_2$ photoluminescence spectra of the solutions under irradiation. (c) Steady state fluorescence emission spectra of the solutions.

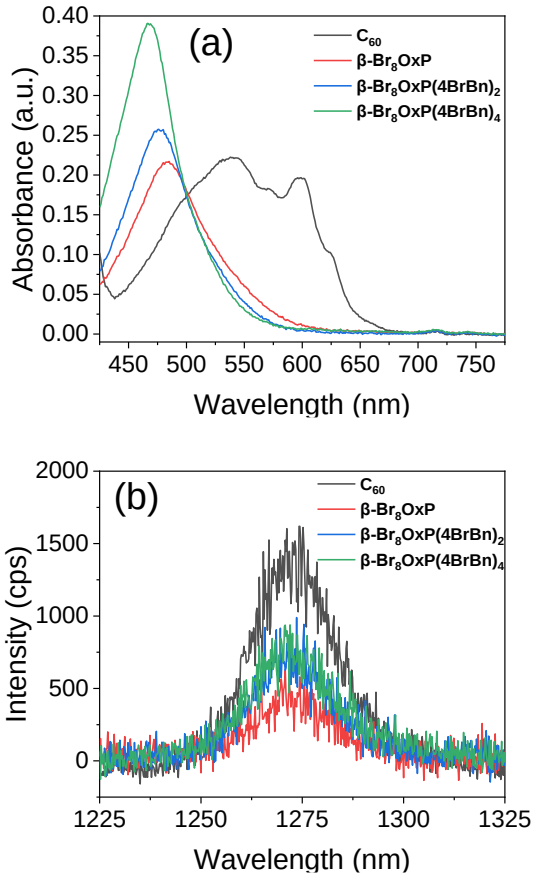

Fig. 5. Electronic absorption and photoluminescence spectra for **β-Br$_8$OxP**, **β-Br$_8$OxP(4BrBn)$_2$** and **β-Br$_8$OxP(4BrBn)$_4$**. (a) UV-vis spectra of solutions of the compounds and reference (C_{60}) having approximately equivalent absorbances at the wavelength of irradiation (500 nm) in toluene. (b) $^1O_2$ photoluminescence spectra of the solutions under irradiation.

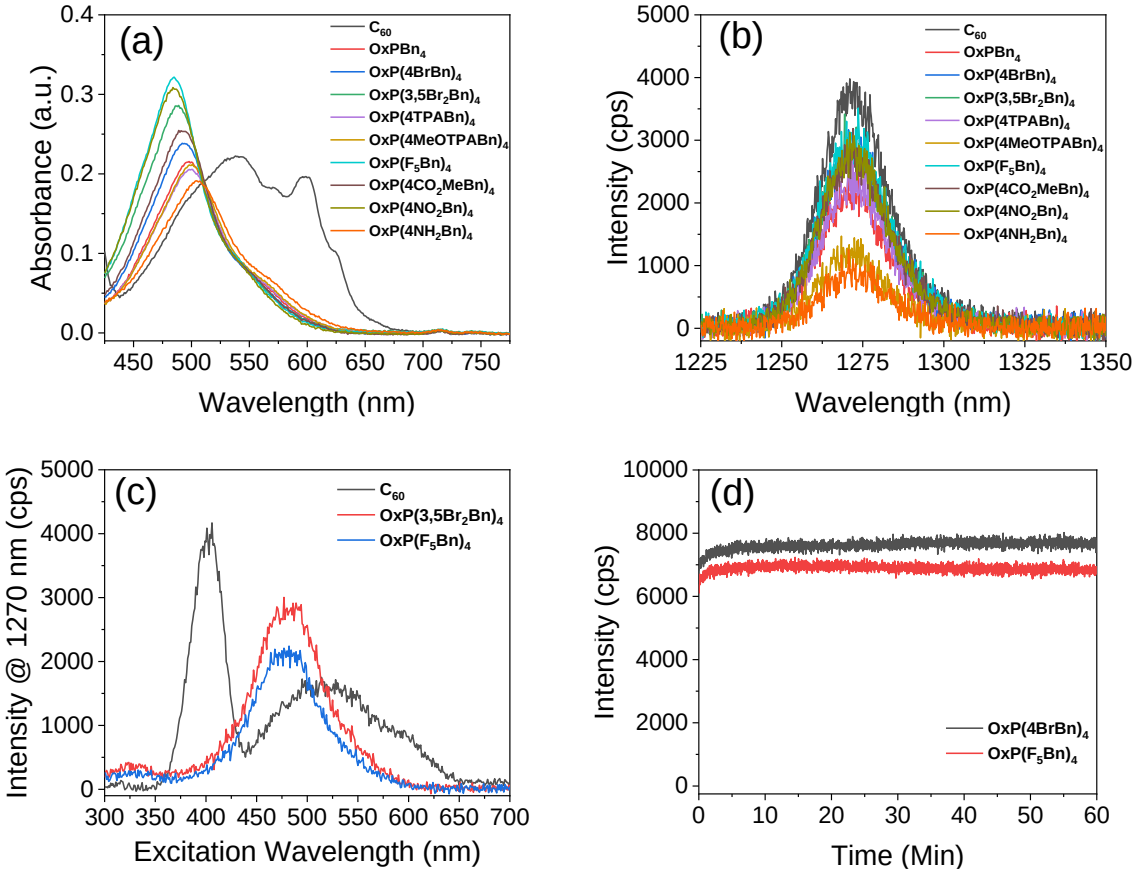

Fig. 6. Electronic absorption and photoluminescence spectra for **OxPBn$_4$**, **OxP(4BrBn)$_4$**, **OxP(3,5Br$_2$Bn)$_4$**, **OxP(4TPABn)$_4$**, **OxP(4MeOTPABn)$_4$**, **OxP(F$_5$Bn)$_4$**, **OxP(4CO$_2$MeBn)$_4$**, **OxP(4NO$_2$Bn)$_4$** and **OxP(4NH$_2$Bn)$_4$**. (a) UV-vis spectra of solutions of the compounds and reference (C_{60}) having approximately equivalent absorbances at the wavelength of irradiation (510 nm) in toluene. (b) $^1O_2$ photoluminescence spectra of the solutions under irradiation. (c) $^1O_2$ excitation spectra of solutions of the indicated compounds under irradiation with monitoring at 1270 nm (d) Chromophore stability profiles of solutions of the indicated compounds under irradiation at 510 nm monitoring at 1270 nm in toluene.

Compound	Emission Intensity @ 1270-1275 nm (c.p.s.)	(Φ_Δ)
OxP	143	0.04
OxP(4BrBn)$_2$	735	0.19
OxP(4BrBn)$_4$	2878	0.75
C$_{60}$ (ref.)[43,44]	3849	1

Table 1. Variation of Φ_Δ with increasing N-substitution of **OxP**.

Compound	Emission Intensity @ 1270-1275 nm (c.p.s.)	(Φ_Δ)
β-Br$_8$OxP	425	0.31
β-Br$_8$OxP(4BrBn)$_2$	687	0.51
β-Br$_8$OxP(4BrBn)$_4$	748	0.55
C$_{60}$ (ref.)[43,44]	1358	1

Table 2. Variation of Φ_Δ with increasing N-substitution of **β-Br$_8$OxP**.

Compound	λ_{max} (nm)	Emission Intensity @ 1270-1275 nm (c.p.s.)	(Φ_Δ)
OxP(4NH$_2$Bn)$_4$	506	879	0.24
OxP(4MeOTPABn)$_4$	500	1193	0.33
OxPBn$_4$	498	2121	0.58
OxP(4TPABn)$_4$	500	2266	0.62
OxP(4CO$_2$MeBn)$_4$	493	2701	0.74
OxP(4NO$_2$Bn)$_4$	485	2770	0.76
OxP(4BrBn)$_4$	494	2829	0.77
OxP(3,5Br$_2$Bn)$_4$	488	2800	0.77
OxP(F$_5$Bn)$_4$	485	2981	0.82
C$_{60}$ (ref.)[43,44]	540	3657	1

Table 3. N-substituent dependency of Φ_Δ for **OxPBn$_4$** arranged in order of increasing quantum yield.